for any i, j, k, could also yield a code based on having all f's odd and all t's odd.

Discussion of the New Orchard Codes

All the codes here could be replaced by their mirror image. Also, all were tested with a computer program to verify their nonambiguity.

The first two codes need about the same number of bits to encode. Decoding requires about twice as many bits as encoding in each case. Both require about a third again as many bits as the Scott and Goetschel code for comparable operations. Correction of the first two new codes could be performed in a conceptually identical fashion [4]. For values of n greater than those listed in Table I, they might be easier to implement, because finding appropriate difference triangles with minimal t_{max} becomes increasingly difficult with large n. Even for tabulated values of n, the symmetry of the patterns would seem to simplify implementation.

The third code needs slightly fewer bits to encode or decode compared to the Scott and Goetschel code for $n < 4$ (and the same at $n = 4$). In that range the smallest SES's are the same and independent of n. This means that the same circuits can be used for $n \leq 4$. Additionally, the number of bits saved will be minimal except for the modified Shiozaki code, which is quite difficult to decode.

Table V indicates the minimum value of t_{max} for the different error correction procedures. To indicate the number of bits saved, one must add 1 and multiply by n, the number of tracks.

In the suggested implementation of the codes [4], the Scott and Goetschel code, and by implication the first two new codes, are easy to correct using combinational logic only. Furthermore, they have good error propagation characteristics. Only a relatively difficult way to decode the Shiozaki code has been suggested [4]. Robinson and Bernstein decoding is of about the same level of difficulty as the Scott and Goetschel codes, but as noted, the code is of minimum distance 4, compared to 5 for all of the others.

Extensions of Orchard Codes

The circular diagrams can be extended to other code designs, if

- all circular diagrams involving a number of nodes smaller than or equal to the sum of the error-correcting and detecting capability of the codes are considered and found to be impossible, and
- each node has as many edges as the SES's have bits.

In all of the cases presented here, any odd number of nodes is impossible with the specification that the nodes have an odd number of edges, so by showing that the four-node case is impossible, the five-node case becomes the largest impossible case. Therefore, the codes will correct two—detect three, or correct one—detect four, or detect five errors.

To investigate a proposal for using difference triangles to create four-bit syndromes for three-error correction, we need to consider five- and six-node cases only. Initial investigations have been made. The number of nodes and branches is manageable if double intercancellation is excluded by orthogonality. However, four-error correction would necessitate an excessive number of nodes and branches for analysis.

Summary

The design and verification of new orchard codes is not difficult with the circular diagram concept. To verify that a proposed code is unambiguous, all that we need to do is make circular diagrams to check that the characteristics of the code preclude realization of the diagrams. The design becomes independent of the number of rows.

TABLE V
MINIMIZED MAXIMUM BIT LENGTH ALONG ANY TRACK FOR VARIOUS ORCHARD CODE DESIGNS, ROBINSON AND BERNSTEIN CODES

Code	t_{max}
Scott and Goetschel	3n, n=4k + 2, n = 4k + 3 3n + 1 otherwise
Shiozaki	$2n + r$, $r \leq \log_2(n+1)$ and odd
New code I	4n or 4n - 1
New code II	4n - 2
New code III	$(n^2 + n + 4)/2$
Robinson and Bernstein*	Selected values [3,4,8] (n=4, length 19), (8,47), (12,146), (16,206), (20,266)
* Minimum distance 4	

To design a new code, we recommend that the circular diagrams be examined for ways to eliminate them, although construction of a new code based entirely on trial-and-error methods is possible, this latter being extremely time consuming, particularly for large n and minimal code length.

References

[1] E. Scott and D. Goetschel, "One check bit per word can correct multibit errors," *Electronics,* pp. 130–134, May 5, 1981.

[2] A. Shiozaki, "Proposal of a new coding pattern in orchard scheme," *Inform. Contr.*, vol. 51, pp. 209–215, 1981.

[3] J. Robinson and A. Bernstein, "A class of binary recurrent codes with limited error propagation," *IEEE Trans. Inform. Theory,* vol. IT-13, pp. 106–113, Jan. 1967.

[4] E. Otter, "The orchard error correcting codes," Ph.D. dissertation, Univ. New Mexico, Albuquerque, Dec. 1984.

[5] W. W. Wu, "Coding for satellite and space channels," *Int. J. Electron.*, vol. 55, pp. 183–212, July 1983.

[6] ——, "New convolutional codes—Part I," *IEEE Trans. Commun.*, vol. COM-23, pp. 942–956, Sept. 1975.

[7] ——, "New convolutional codes—Part II," *IEEE Trans. Commun.*, vol. COM-24, pp. 19–32, Jan. 1976.

[8] E. Klieber, "Some difference triangles for constructing self-orthogonal codes," *IEEE Trans. Inform. Theory,* vol. IT-16, pp. 237–238, Dec. 1961.

Spread-Spectrum Despreading Without the Code

C. A. FRENCH AND W. A. GARDNER

Abstract—**A new method for despreading direct-sequence spread-spectrum signals, without use of the spreading code, is evaluated by analysis and simulation. The new method exploits the cyclic autocorrelation in place of the conventional autocorrelation, which was used in a prior method. Both methods require that the period of the code be equal to a multiple of the data symbol interval. Broad-band noise and narrow-**

Paper approved by the Editor for Data Communication and Modulation of the IEEE Communications Society. Manuscript received January 14, 1985; revised August 12, 1985.

C. A. French is with the Department of Electrical Engineering and Computer Sciences, University of California at San Diego, La Jolla, CA 92093.

W. A. Gardner is with the Department of Electrical and Computer Engineering, University of California, Davis, CA 95616.

IEEE Log Number 8607739.

band interference rejection capabilities of both methods are compared. It is shown that the new method, unlike the prior method, can provide substantial immunity to strong narrow-band interference.

I. Introduction

Despreading a direct-sequence spread-spectrum signal without knowledge of the pseudonoise (PN) spreading sequence (also known as blind despreading) can be accomplished, provided that a few parameters of the signal are known. In this paper, the case of interest is that in which the BPSK carrier frequency, the data rate, and the PN code repetion rate are known. Furthermore, it is assumed that the repetition rate of the PN sequence is a small integer multiple of the data rate. The simulation results in Section IV use a code repetition rate exactly equal to the data symbol rate.

A previously proposed method of blind despreading for direct sequence BPSK signals uses a type of autocorrelation, and will be referred to as the *conventional autocorrelation method*. This method correlates the incoming signal with a delayed version of itself, where the delay is equal to the repetition period of the spreading code. If the received waveform consists of the spread-spectrum signal plus additive broad-band noise, the signal and its delayed version will be highly correlated, while the noise will be uncorrelated with a delayed version of itself and of the signal. Unfortunately, however, the autocorrelation operation multiplies the undesirable noisy portion of the received waveform by itself. If narrow-band interference is present as well, the autorcorrelation operation demodulates the interference into the demodulated signal band, where it interferes with signal detection.

The new method of blind despreading proposed here has interference rejection capabilities that greatly improve on the performance of the prior method. This new method uses a type of cyclic autocorrelation, and is therefore referred to as the *cyclic autocorrelation method*.[1] This method compares the incoming corrupted signal with a delayed version of itself (as in the autocorrelation method) *and* jointly with a sinusoid of frequency $2f_0$, where f_0 is the carrier frequency of the BPSK spread-spectrum signal. The introduction of this sinusoid in the autocorrelation operation has the effect of shifting narrow-band interference out of the demodulated signal band, as long as the center frequency of the interference is not too close to the BPSK carrier frequency, relative to the unspread signal bandwidth. Broad-band noise rejection for the cyclic autocorrelation method is comparable to that described for the conventional autocorrelation method, due again to the self-multiplication effect of the autocorrelation operation on the noise.

Descriptions of the spread-spectrum signal of interest, and of the two blind despreading methods considered, are given in Section II. Theoretical comparisons of the two methods are presented in Section III. Finally, computer simulation results are given in Section IV to support the theoretical results.

II. Despreading Without the Code

Consider a series of data bits, d_n, taking values ± 1, where d_1 is the first bit, d_2 is the second bit, etc. These bits can be converted into a binary PAM waveform with time-samples denoted by $D(jT_s)$, where T_s is the time between discrete points (the sampling time) and j is the time index.[2] The data period T_d is assumed to be much greater than the sampling time. If a pseudorandom discrete-time waveform $C(jT_s)$ (taking values ± 1), with a chip interval of T_c seconds (assumed to be much smaller than T_d), which repeats every P data periods, is used to multiply the data, a binary PN spread-spectrum baseband signal results and is given by

$$B(jT_s)=D(jT_s)C(jT_s). \tag{1}$$

The spread-spectrum signal of interest is obtained by modulating the amplitude (or equivalently, the phase) of a sinewave with the baseband spread data sequence $B(jT_s)$. This yields the BPSK signal

$$S(jT_s)=B(jT_s)\ \cos\ (2\pi f_0 jT_s+\phi_0). \tag{2}$$

In general, the received signal will be masked by noise and interference, and therefore, the input to the receiver is modeled as

$$X(jT_s)=S(jT_s)+I(jT_s)+N(jT_s) \tag{3}$$

where $S(jT_s)$ is as defined in (2), $I(jT_s)$ is a narrow-band interference term given by the idealized (zero-bandwidth) form

$$I(jT_s)=A_i\ \cos\ (2\pi f_i jT_s+\phi_i) \tag{4}$$

and $N(jT_s)$ is a band-limited white Gaussian noise term with power spectral density given by

$$S_N(f)=\begin{cases} N_0, & 0<\|f|-f_0|<1/T_c \\ 0, & \text{otherwise.}\end{cases} \tag{5}$$

The cyclic autocorrelation of the corrupted spread-spectrum signal evaluated at a lag of PT_d is defined by

$$R_X^{\alpha}(jT_s,\ PT_d)=\frac{1}{T_d}\sum_{k=0}^{T_d/T_s-1} X(jT_s-kT_s)$$

$$\cdot\ X(jT_s-kT_s-PT_d)\ \cos\ (2\pi\alpha kT_s+\theta) \tag{6}$$

where the cycle parameter α takes on a value of $2f_0$ for the BPSK spread-spectrum signal defined previously. For $\alpha = 0$, (6) reduces to the conventional autocorrelation of $X(jT_s)$. Manipulation of (6) suggests the implementations shown in Fig. 1. For details of this manipulation, the interested reader is referred to [1]. The outputs of the despreaders in Fig. 1 are differentially encoded versions of the input data bits. Practical considerations such as differential decoding of outputs, synchronization to the data rate for sampling (for both despreading methods), and synchronous detection (for the cyclic method) are briefly discussed in [1].

III. Theoretical Performance

One method of comparing the theoretical performance of the conventional and cyclic autocorrelation despreaders is to compare their output signal-to-noise ratios (SNR) and signal-to-interference ratios (SIR), or equivalently, their SNR and SIR gains (i.e., SNR gain = $\mathrm{SNR_{out}/SNR_{in}}$). Input SNR and SIR are defined as

$$\mathrm{SNR_{in}}=\frac{\int_{-\infty}^{\infty} S_S(f)\ df}{\int_{-\infty}^{\infty} S_N(f)\ df} \tag{7a}$$

and

$$\mathrm{SIR_{in}}=\frac{\int_{-\infty}^{\infty} S_S(f)\ df}{\int_{-\infty}^{\infty} S_I(f)\ df} \tag{7b}$$

respectively, where $S_S(f)$ is the power spectral density of the

[1] The cyclic autocorrelation method of blind despreading originated from the theory of cyclic autocorrelation developed in [2], [3].

[2] In anticipation of the computer simulation as well as possible digital implementations for sufficiently low-frequency applications, all quantitites are expressed in discrete-time form.

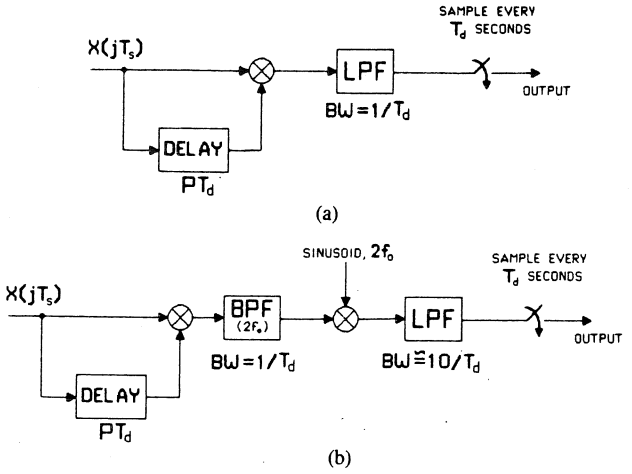

Fig. 1. (a) Conventional autocorrelation despreader. (b) Cyclic autocorrelation despreader.

input signal, $S_N(f)$ is the power spectral density of the input noise [defined in (5)], and $S_I(f)$ is the power spectral density of the zero-bandwidth interference. Output SNR and SIR (before sampling) are defined as

$$\mathrm{SNR}_{\mathrm{out}} = \frac{\int_{-\infty}^{\infty} S_{SS}(f)\ df}{\int_{-\infty}^{\infty} S_{NN}(f)\ df} \tag{8a}$$

and

$$\mathrm{SIR}_{\mathrm{out}} = \frac{\int_{-\infty}^{\infty} S_{SS}(f)\ df}{\int_{-\infty}^{\infty} S_{II}(f)\ df} \tag{8b}$$

respectively, where $S_{SS}(f)$ is the portion of the output power spectral density of the despreader due only to signal–signal interactions, $S_{NN}(f)$ is the portion of the output power spectral density of the despreader due only to noise–noise interactions, and $S_{II}(f)$ is the portion of the output power spectral density of the despreader due only to interference–interference interactions. The output power spectral density of either despreader in Fig. 1 has other terms due to signal–noise, signal–interference, and noise–interference interactions. Contributions of these crossterms can be significant, and they are considered in [1].

Using definitions 7 and 8, expressions for input and output SNR and SIR, as well as SNR and SIR gain were derived for the conventional and cyclic autocorrelation despreaders. Derivations can be found in [1], and the results are summarized in Table I.

From Table I it is clear that SNR gains for the two despreaders are of the same form and same order of magnitude (since the factor $\cos^2(2\pi f_0 PT_d)$ is typically unity). Note that SNR gain for both blind despreading methods is also proportional to the input SNR, due to the noise–multiplication effect of the autocorrelation operations. Therefore, for $\mathrm{SNR}_{\mathrm{in}} < 1$, which is typically the case, these blind despreading methods exhibit low tolerance to broad-band noise if the spreading gain factor T_d/T_c is not sufficiently large.

Referring to the SIR gains in Table I, it appears that interference rejection for the blind despreaders might be poor, since SIR gain is proportional to input SIR (which can be less than 1) for these two methods. However, the equations for SIR gain reveal that the cyclic autocorrelation despreader should reject interference better than the conventional autocorrelation

TABLE I
SNR AND SIR FOR BLIND DESPREADING

	Conventional	Cyclic
$\mathrm{SNR}_{\mathrm{in}}$	$\frac{T_c}{8N_o}$	$\frac{T_c}{8N_o}$
$\mathrm{SNR}_{\mathrm{out}}$	$\frac{8T_d}{3T_c}\cos^2(2\pi f_o PT_d)\,\mathrm{SNR}_{\mathrm{in}}^2$	$\frac{4T_d}{3T_c}\mathrm{SNR}_{\mathrm{in}}^2$
$\frac{\mathrm{SNR}_{\mathrm{out}}}{\mathrm{SNR}_{\mathrm{in}}}$	$\frac{8T_d}{3T_c}\cos^2(2\pi f_o PT_d)\,\mathrm{SNR}_{\mathrm{in}}$	$\frac{4T_d}{3T_c}\mathrm{SNR}_{\mathrm{in}}$
$\mathrm{SIR}_{\mathrm{in}}$	$\frac{1}{A_i^2}$	$\frac{1}{A_i^2}$
$\mathrm{SIR}_{\mathrm{out}}$	$\frac{2\cos^2(2\pi f_o PT_d)}{3\cos^2(2\pi f_i PT_d)}\mathrm{SIR}_{\mathrm{in}}^2$	$\frac{2}{3}\mathrm{sinc}^{-2}[2T_d(f_o-f_i)]\,\mathrm{SIR}_{\mathrm{in}}^2$
$\frac{\mathrm{SIR}_{\mathrm{out}}}{\mathrm{SIR}_{\mathrm{in}}}$	$\frac{2\cos^2(2\pi f_o PT_d)}{3\cos^2(2\pi f_i PT_d)}\mathrm{SIR}_{\mathrm{in}}$	$\frac{2}{3}\mathrm{sinc}^{-2}[2T_d(f_o-f_i)]\,\mathrm{SIR}_{\mathrm{in}}$

despreader, due to the factor

$$\mathrm{sinc}^{-2}\ [2T_d(f_0 - f_i)]. \tag{9}$$

This factor reveals that interference rejection for the cyclic autocorrelation method improves as the center frequency of the interference moves away from the carrier frequency of the spread-spectrum signal, and that it is the separation of these two frequencies relative to the unspread signal bandwidth, $1/T_d$, that is the controlling quantity.

IV. Simulation Results

Fig. 2 shows time waveform outputs of a computer simulation of the conventional and cyclic autocorrelation despreaders, to demonstrate qualitatively how the despreaders perform in the presence of interference and noise. Table II(a) gives the parameters used in the simulation. 10 data bits are shown for each case in Fig. 2, and the tick marks indicate where sampling should occur. Clearly, the cyclic autocorrelation method outperforms the conventional autocorrelation method when strong narrow-band interference is present [see Fig. 2(d)].

Input SNR tolerance was measured with a second run of the simulation (see Table II(b) for parameters used). With no narrow-band interference present, the input SNR was decreased until two or more errors in 30 bits occurred. At this error rate, both blind despreading methods could tolerate an input SNR as low as about -15 dB, while an input SNR of about -30 dB could be tolerated if despreading were done using the PN code.

Another run of the simulation (see Table II(b) for parameters used) was used to measure tolerable input SIR for an output error rate of less than two errors in 30 bits. A narrow-band interference term was added to a signal already corrupted with broad-band noise (i.e., $\mathrm{SNR}_{\mathrm{in}} = -10$, 0, or $+10$ dB). Various interference frequencies throughout the signal band were tested, with three data points (from three statistical samples) taken at each interference frequency for a given $\mathrm{SNR}_{\mathrm{in}}$. These points were averaged to obtain the plot of Fig. 3. Three points in the average was considered adequate since their spread was relatively small. Data for despreading using the PN code for $\mathrm{SNR}_{\mathrm{in}} = -10$ dB is included for comparison.

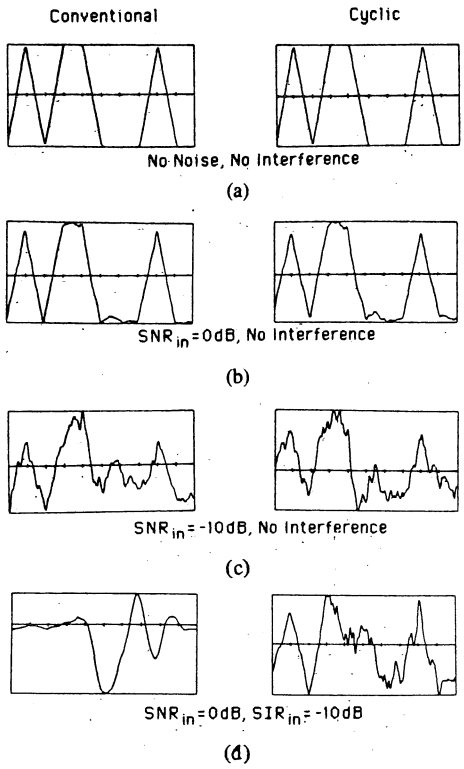

Fig. 2. Time waveform outputs from simulation.

TABLE II
SIMULATION PARAMETERS

	(a) Version 1	(b) Version 2
Number of bits	10	30
T_d(sec)	$800T_s$	$3200T_s$
T_c(sec)	$8T_s$	$32T_s$
P	1	1
f_o(Hz)	$\frac{1}{8T_s}$	$\frac{1}{8T_s}$
ϕ_o(radians)	0.79	0.79
f_i(Hz)	$\frac{1}{11.5T_s}$	—
ϕ_i(radians)	0.5	0.5

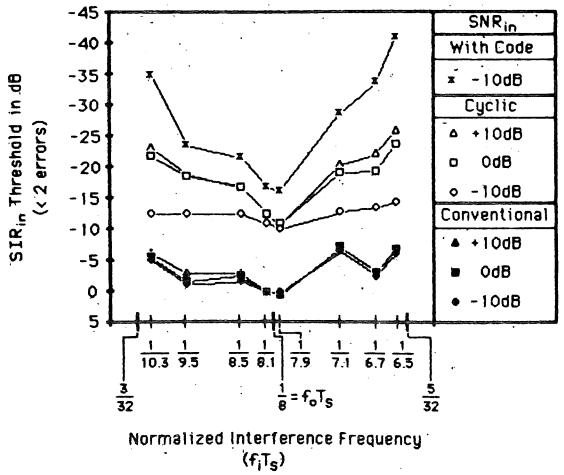

Fig. 3. Averaged input SIR threshold for one interferer.

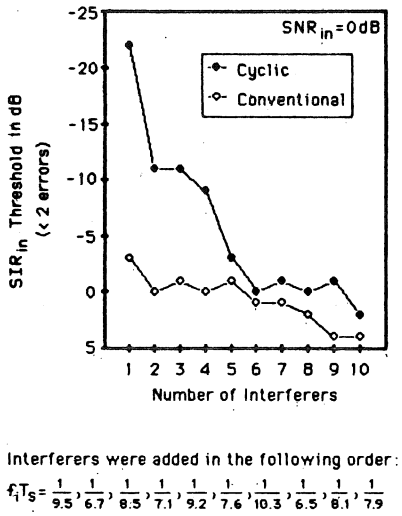

Fig. 4. Input SIR threshold versus number of interferers.

Fig. 3 again indicates the superiority of the cyclic autocorrelation despreader over the conventional autocorrelation despreader in interference rejection.

In a final experiment, ten different interferers centered at various frequencies throughout the spread-spectrum band were added, one at a time, to the spread-spectrum signal, with input SNR held at 0 dB. Input SIR threshold (for one or fewer errors in a string of 30 data bits) was determined for both blind despreading methods after the addition of each interferer, with the results shown in Fig. 4. For a given number of interferers, input SIR was made the same for all interference frequencies. It appears in Fig. 4 that five or six interferers are required before the performance of the cyclic autocorrelation despreader degrades to about the same performance level as the conventional autocorrelation despreader.

V. Summary

The theoretical performance formulas in Section III, and both the qualitative performance comparisons based on time waveforms and the quantitative results presented in Section IV indicate that the cyclic autocorrelation despreader is superior to the conventional autocorrelation despreader for interference rejection. For a spreading gain factor of $T_d/T_c = 100$, and depending on the amount of broad-band noise present, the cyclic autocorrelation method can tolerate a 10–15 dB lower input SIR than the conventional autocorrelation method (see Fig. 3).

As expected, both blind despreading methods failed at higher input SNR and SIR than when the corrupted signal was despread using the PN code. As long as an autocorrelation is used (as required for blind despreading when the code is unavailable), the noise-multiplication effect is unavoidable.

Although the implementation required for the cyclic autocorrelation despreading method is more complex than that for the conventional autocorrelation method (requiring an additional filter and a modulator which requires synchronization), the benefits in interference rejection of the cyclic autocorrelation method could prove to be significant in certain applications.

References

[1] C. A. French, "Spread spectrum despreading without the code," M.S. thesis, Dep. Elec. Comput. Eng., Univ. California, Davis, Sept. 1984.

[2] W. A. Gardner, *Introduction to Random Processes with Applications to Signals and Systems.* New York: Macmillan, 1985.

[3] ——, "Statistical spectral analysis: A nonprobabilistic theory. Part II: Periodic phenomena," Signal and Image Processing Lab., Dep. Elec. Comput. Eng., Univ. California, Davis, Rep. SIPL-83-6, Sept. 1983.

On the Spectrum of Pseudo Noise

W. A. GARDNER AND C-K. CHEN

Although the magnitude of the discrete Fourier transform of a maximal-length shift-register sequence is flat, except for its value at zero frequency, the higher resolution spectral content given by the Fourier-series transform is highly erratic. This little-known fact is described, and its ramifications on fast Fourier transforms of one-digit-extended pseudo noise and zero-padded pseudo noise are explained.

A *pseudo noise* (PN) sequence is a sequence of numbers, most commonly +1s and −1s (or 1s and 0s), that appears to be random but in fact is perfectly predictable given the algorithm that generates it. A particularly important type of PN sequence is the *maximal-length shift-register sequence*, which when periodically repeated yields a limit autocorrelation sequence that is similar to that for white noise. The limit autocorrelation sequence is defined by

$$R_x(k) \triangleq \lim_{Q\to\infty} \frac{1}{2Q+1} \sum_{n=-Q}^{Q} x_{n+k}x_n \tag{1}$$

and for a periodic sequence with period N we have

$$R_x(k) = \frac{1}{N}\sum_{n=0}^{N-1} x_{n+k}x_n = R_x(k+N). \tag{2}$$

The sequence given by (2) is called the *circular autocorrelation* of the periodic sequence $\{x_n\}$. For a maximal length sequence $\{x_n\}$, it can be shown [1] that

$$R_x(k) = \begin{cases} 1, & k = 0 \\ -1/N, & 1 \leqslant |k| \leqslant N-1 \end{cases} \tag{3}$$

where $N = 2^M - 1$ for some positive integer M. Thus $R_x(k)$ approaches the limit autocorrelation for white noise as $N \to \infty$. It is well known that the N-point discrete Fourier transform (DFT) of a circular autocorrelation of a periodic sequence with period N is given by

$$\text{DFT}\{R_x(k)\} \triangleq \sum_{k=0}^{N-1} R_x(k)e^{-i2\pi km/N}, \qquad m = 0,1,2,\cdots,N-1 \tag{4}$$

$$= \frac{1}{N}\left|\sum_{n=0}^{N-1} x_n e^{-i2\pi nm/N}\right|^2 \tag{5}$$

$$\triangleq \frac{1}{N}|\text{DFT}\{x_n\}|^2 \tag{6}$$

and also that (3) can be used to show that

$$\text{DFT}\{R_x(k)\} = \begin{cases} 1/N, & m = 0 \\ 1 + 1/N, & 1 \leqslant |m| \leqslant N-1. \end{cases} \tag{7}$$

Now, let us consider the DFT $\{X_m\}$ of the maximal length sequence $\{x_n\}$ itself, rather than the DFT of its autocorrelation sequence. It follows from (6) and (7) that the magnitude of the DFT $\{X_m\}$ of a maximal-length sequence $\{x_n\}$ is given by

$$|X_m| = \begin{cases} 1, & m = 0 \\ \sqrt{N+1}, & 1 \leqslant |m| \leqslant N-1 \end{cases} \tag{8}$$

which is flat except for a notch at zero frequency, as shown in Fig. 1(a).

The Fourier series transform (FST) of a sequence $\{x_n\}$ is defined by

Manuscript received July 23, 1985; revised August 30, 1985.

The authors are with the Signal and Image Processing Laboratory, Department of Electrical and Computer Engineering, University of California at Davis, Davis, CA 95616, USA.

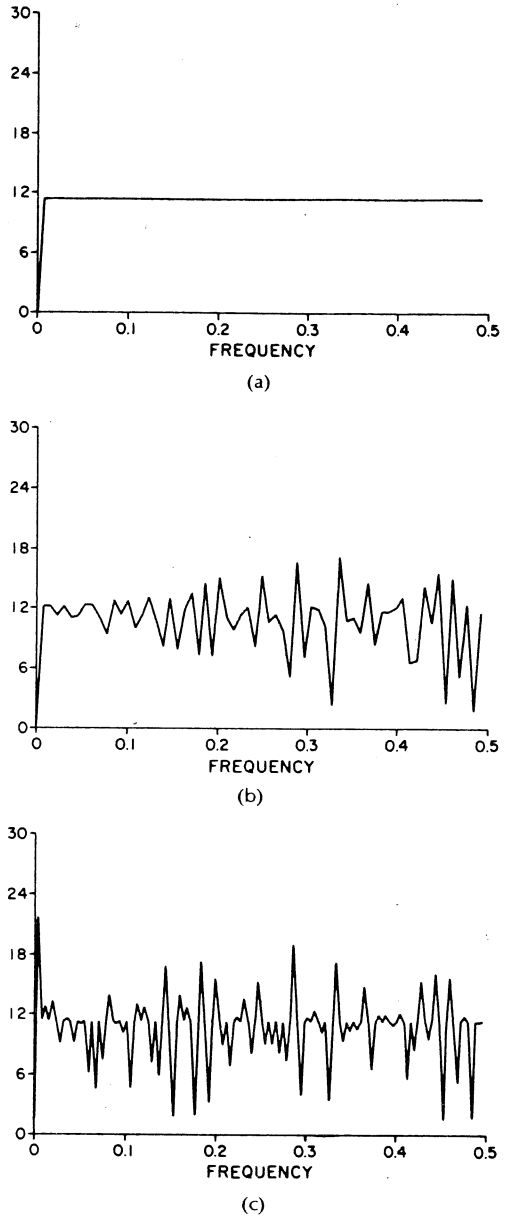

Fig. 1. Magnitudes of DFTs of a ±1 maximal-length shift-register sequence of length $N=127$. (Data points connected by straight lines.) (a) Original sequence. (b) One digit-extended sequence with length $N'=128$. (c) Zero-padded sequence with length $N'=254$.

$$X(f) \triangleq \sum_{n=0}^{N-1} x_n e^{-i2\pi fn}, \qquad |f| \leqslant 1/2 \tag{9}$$

from which it follows that the DFT is simply the sampled FST

$$X_m = X(m/N). \tag{10}$$

Furthermore, it is well known that the FST $X(f)$ can be obtained from the DFT $\{X_m\}$ by interpolation, and since the DFT of $\{x_n\}$, zero-padded out to length $N' = KN$ to produce (say) $\{Y_n\}$, is

$$Y_m = X(m/KN) \tag{11}$$

then the DFT $\{Y_m\}$ of the zero-padded sequence can also be obtained from $\{X_m\}$ by interpolation. The interpolation formula is easily shown to be

$$Y_m = \sum_{p=0}^{N-1} X_p I(p - m/K) \tag{12a}$$

0018-9219/86/0400-0608$01.00

where the interpolation function is given by

$$|I(q/K)| = \frac{\sin(\pi q/K)}{\sin(\pi q/KN)} \tag{12b}$$

$$\arg\{I(q/K)\} = (\pi q/K)(1 - 1/N). \tag{12c}$$

If one extra digit, say -1, is added to a PN sequence in order to obtain an integer-power-of-two for the sequence length $N' = N + 1 = 2^M$, then an FFT algorithm can be used to compute the DFT. The DFT of the one-digit-extended PN sequence

$$z_n = \{x_0, x_1, x_2, \cdots, x_{n-1}, -1\} \tag{13}$$

is given by

$$Z_m \triangleq \sum_{n=0}^{N} z_n e^{-i2\pi nm/(N-1)} \tag{14}$$

$$= \sum_{n=0}^{N-1} x_n e^{-i2\pi nm/(N+1)} - e^{-i2\pi mN/(N+1)}$$

$$= X\left(\frac{m}{N+1}\right) - e^{-i2\pi mN/(N+1)}$$

$$= X\left(\frac{m}{N} - \frac{m}{N(N+1)}\right) - e^{-i2\pi mN/(N+1)}. \tag{15}$$

For large N, the exponential term is negligible except at $m = 0$ (cf. (8)), and Z_m is, therefore, closely approximated by the FST $X(f)$ sampled at points that are slightly offset from the samples that yield X_m, (10). This same result is obtained regardless of the position of the extra digit among the original N digits.

Considering the flatness of the DFT magnitude $\{|X_m|\}$, one would expect both the one-digit-extended DFT magnitude $\{|Z_m|\}$ and the zero-padded DFT magnitude $\{|Y_m|\}$ to be very nearly flat. But this is not the case. For example, these three DFT magnitudes are shown in Fig. 1(a), (b), (c) for a maximal-length shift-register sequence of length $N = 127$, and it can be seen that both $\{|Z_m|\}$ and $\{|Y_m|\}$ are highly erratic. The reason for this is that the FST $X(f)$ is highly erratic, as shown in Fig. 2, and the reason for this is that

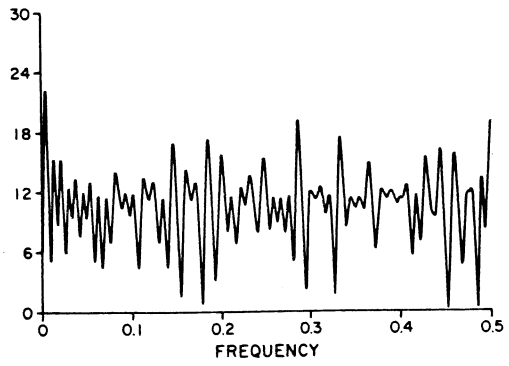

Fig. 2. Magnitude of the FST (actually DFT zero padded out to length 4096) of the ± 1 maximal-length shift-register sequence of length 127, whose DFT magnitude is shown in Fig. 1(a). (Data points connected by straight lines.)

although $X(f)$ is an interpolated version of the DFT $\{X_m\}$, whose magnitude is flat, the phase of $\{X_m\}$ is highly erratic, as shown in Fig. 3. OF course, even though $X(f)$ is highly erratic, its samples $X_m = X(m/N)$ do have constant magnitude (for $m \neq 0$) as required by (8).

Since the FST of a PN sequence is not at all flat, this brings into question the idea that a PN sequence is similar to white noise. However, the FST of white noise is also a highly erratic function. It is only after smoothing that it approximates the ideal average power spectral density which is flat. As a matter of fact, a PN sequence is indeed similar to white noise since its highly erratic FST

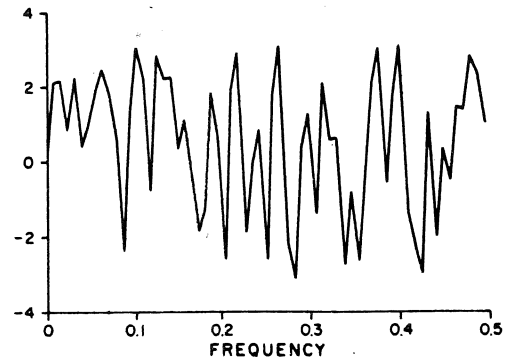

Fig. 3. Phase of the DFT of the ± 1 maximal-length shift-register sequence of length $N = 127$, whose DFT magnitude is shown in Fig. 1(a). (Data points connected by straight lines.)

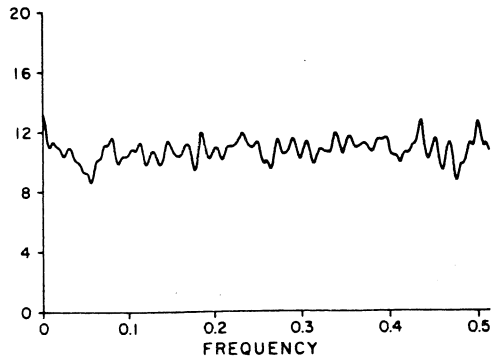

Fig. 4. Smoothed magnitude of the FST shown in Fig. 2. Smoothing-window width is 100 points, which is approximately 3 bins from the DFT of the nonzero-padded sequence. (Data points connected by straight lines.)

closely approximates a flat spectrum when it is smoothed as shown in Fig. 4. The smoothing window used here is 100 points wide, and the total number of transform points is 4096. Thus approximately 3 bins from the original (nonzero-padded) 127-point DFT are averaged.

In summary, although one might expect the DFT of one-digit-extended pseudo noise, and the DFT of zero-padded pseudo noise, to be nearly flat, these DFTs are in fact highly erratic, and this confirms the idea that pseudo noise is similar to white noise.

References

[1] S. W. Golomb, *Shift Register Sequences*. San Francisco, CA: Holden-Day, 1967.

Performance of Adaptive Filters Using Combined Lattice and Transform Techniques

JOHN S. SOUNDARARAJAN AND
N. B. CHAKRABORTI

A composite scheme combining lattice and transform techniques for implementation of adaptive filters is discussed. Results of the eigenvalue spreads and convergence time for simple correlation cancelers in combination with Walsh–Hadamard Transform (WHT) are reported.

Manuscript received June 20, 1985; revised September 19, 1985.

The authors are with the Department of Electronics and Electrical Communication Engineering, Indian Institute of Technology, Kharagpur 721 302, W.B., India.

0018-9219/86/0400-0609$01.00 ©1986 IEEE